



# Three-dimensional human skin model infected with *Staphylococcus aureus* as a tool for evaluation of bioactivity and biocompatibility of antiseptics

Kirsten Reddersen\*, Cornelia Wiegand, Peter Elsner, Uta-Christina Hipler

Department of Dermatology, University Hospital Jena, Jena, Germany

## ARTICLE INFO

### Article history:

Received 4 April 2019

Accepted 28 June 2019

Editor: Stefania Stefani

### Keywords:

3D infected skin model

Antiseptics

*Staphylococcus aureus*

Immune response

## ABSTRACT

In the light of pandemic spreads of multi-drug-resistant micro-organisms, alternative antimicrobial strategies to the use of antibiotics are the focus of research attention. As a prerequisite for medical application, the aim of this study was to develop a three-dimensional full skin infection model to evaluate the bioactivity and biocompatibility of antiseptics in application-relevant concentrations. A three-dimensional (3D) full skin model consisting of collagen-embedded fibroblasts as dermis and a fully differentiated epidermis built from keratinocytes was infected with *Staphylococcus aureus*. Infected skin models were treated for 24 h with the antiseptics polihexanide, octenidine dihydrochloride, chlorhexidine digluconate and povidone-iodine. Infection resulted in detrimental effects, a strong immune response with increased secretion of lactate dehydrogenase and pro-inflammatory cytokines, and increased gene expression of pro-inflammatory cytokines and antimicrobial peptides after 24 h. Application of antiseptics protected the skin models from damage due to *S. aureus* infection while demonstrating good biocompatibility. The best ratio of bioactivity to biocompatibility was observed for polihexanide. Polihexanide also enhanced the innate immune response by increasing the gene expression levels of antimicrobial peptides such as human  $\beta$ -defensin 2, human  $\beta$ -defensin 3, psoriasin and ribonuclease 7. The developed model provides an excellent tool to investigate the response of human cells to microbial infections in a complex 3D structure. Furthermore, the infection model is appropriate for evaluation of bioactivity and biocompatibility of antiseptics. As such, the model presented in this study is a promising approach to evaluate the mechanisms and effectiveness of new antimicrobial strategies.

© 2019 Elsevier B.V. and International Society of Chemotherapy. All rights reserved.

## 1. Introduction

Topical antiseptics play a key role in preventing nosocomial infections as well as treating acute and chronic wounds [1]. However, the evaluation of bioactivity and cell compatibility is often carried out in separate studies. On the one hand, antiseptic efficacy is determined with planktonic bacteria such as *Staphylococcus aureus*, *Pseudomonas aeruginosa*, *Escherichia coli*, *Streptococcus pneumoniae* and *Clostridium perfringens* [2]. On the other hand, biocompatibility is tested with monolayer cultures of keratinocytes, fibroblasts, thyroid cancer cells and epithelial cells [3–7]. Only a few studies have combined the assessment of bioactivity and biocompatibility of antiseptics, either in parallel [1,8,9] or in co-culture models [10]. There are further major limitations for testing antiseptics in

two-dimensional (2D) models, such as communication between the cell and its matrix or adjacent cells and the interplay between different cell types are not accounted for when culturing cells in two dimensions [11]. Cells react more sensitively in 2D monolayers compared with complex 3D cell structures where cell-to-cell interactions between different cell types take place [12]. In accordance, the concentration range for testing antiseptics in 2D models is significantly lower than application-relevant amounts [3,5,7,8].

Cells and micro-organisms need to be investigated in more complex model systems to improve in-vitro to in-vivo extrapolation of test results. A number of studies on microbial colonization using 3D epidermal models have been published to date. These commercially available or in-house epidermal models consist of differentiated keratinocytes on an artificial membrane. The skin models provide the same specific conditions as human skin for bacteria to attach to the surface because of formation of a stratum corneum [13]. Adhesion and colonization of *S. aureus*, *P. aeruginosa*, *Staphylococcus epidermidis*, *Acinetobacter baumannii* and *Acinetobacter junii* have been studied using 3D epidermal models [13–16].

\* Corresponding author. Address: Department of Dermatology, University Hospital Jena, Erfurter Strasse 35, 07743 Jena, Germany. Tel.: +49 3641 937386; fax: +49 3641 937437.

E-mail address: [kirsten.reddersen@med.uni-jena.de](mailto:kirsten.reddersen@med.uni-jena.de) (K. Reddersen).

Only a few of these studies combined microbial colonization of the epidermal models with testing of antiseptic strategies. Mueller et al. [14] used an in-house epidermal model to study the residual antimicrobial activity of chlorhexidine and octenidine against *S. aureus* and *P. aeruginosa* after topical exposure for 15 min. De Breij et al. [13] studied the eradication of *A. baumannii* from an in-house epidermal model by chlorhexidine. However, none of these studies employed different cell types that are present in human skin. To reflect a more in-vivo-like situation, 3D full skin models can be used. These models feature a dermal layer with fibroblasts and an epidermal layer with differentiated keratinocytes. Full skin models have been used to investigate the colonization of a variety of micro-organisms: *S. aureus*, *S. epidermidis*, *Propionibacterium acnes* and *Malassezia furfur* [17–20]. However, none of the approaches to date have investigated the interaction of different skin cells, microbes and antiseptics in one in-vitro model. Little information is currently available on the interaction of human skin cells in a complex environment and antiseptics following bacterial infection.

Therefore, the aim of this study was to develop a 3D full skin model infected with *S. aureus* to generate a reliable tool to investigate bioactivity and biocompatibility of antiseptics in application-relevant concentrations.

## 2. Material and methods

### 2.1. Generation of 3D skin equivalents

Three-dimensional skin models were cultured according to Wiegand et al. [21]. Minor alterations were applied. Keratinocytes were seeded at day 8, and models were cultured submerged for 10 days and air lifted for 10 days. Prior to the infection experiments, the last two media changes were performed without gentamicin.

### 2.2. Preparation of the bacterial suspension

*S. aureus* ATCC 6538 (DZMZ, Braunschweig, Germany) was incubated on Columbia agar plates (biomérieux, Marcy l'Etoile, France) overnight at 37°C. Bacteria were suspended in tryptic soy broth (Oxoid, Basingstoke, UK) and cultivated for 24 h at 37°C under vigorous shaking. The bacterial suspension was washed twice in 0.9% NaCl. The number of bacteria in the solution was determined by serial dilution followed by plating on Columbia agar. After 24 h of incubation at 37°C, colonies were counted and microbial count (in colony-forming units/mL) of the bacterial suspension was calculated.

### 2.3. Infection and antibacterial treatment of the 3D skin equivalents

The 3D skin equivalents were infected with 5  $\mu$ L of a  $1 \times 10^9$  colony-forming units/mL suspension of *S. aureus*. Five microlitres of NaCl was added to non-infected control models. Microbial density was determined in previous experiments (data not shown) to cause significant damage to the skin models after 24 h of incubation. After 1 h, the infected models were treated with the following antiseptics: chlorhexidine digluconate 0.2% (CHX, Sigma, St Louis, MO, USA), polihexanide 0.02% (PHMB, Fagron, Rotterdam, The Netherlands), octenidine dihydrochloride 0.01% (OCT, Schülke, Norderstedt, Germany) and povidone-iodine 1% (PVP-IOD, Mundipharma, Cambridge, UK). Concentrations of the antiseptics in these studies were chosen according to the range of clinical applications on skin. Deionized water as antiseptic diluent, antiseptics without previous infection, and 1% SDS were included as controls. Sampling was carried out 24 h after treatment. Supernatants were collected and stored for analysis of cytokine levels at -20°C until analysis. Skin models were transferred to 4% formalin solution (Dr K. Hollborn &

Söhne, Leipzig, Germany) for histology or used for RNA isolation to analyse gene expression.

### 2.4. Determination of antibacterial activity

Microbial burden after incubation was determined by rinsing the skin models with  $5 \times 1$  mL 0.2% Tween 20 (Carl Roth GmbH, Karlsruhe, Germany) in phosphate buffered saline (Carl Roth GmbH). The combined rinsing solutions were serially diluted and plated on Columbia agar (biomérieux). After 24 h of incubation at 37°C, colonies were counted and the microbial burden of the skin models was calculated.

### 2.5. Determination of cytotoxicity

Cytotoxic effects of bacteria and antiseptics on the skin models were determined by measuring the activity of lactate dehydrogenase (LDH) in the surrounding media using a cytotoxicity detection kit (Roche, Basel, Switzerland). Due to cell damage following necrotic cell death, LDH is released to the medium. The assay was run as recommended by the manufacturer. A plate photometer was used to measure optical density at 490 nm (POLARstar Galaxy, BMG Labtech GmbH, Ortenberg, Germany). LDH release during infection and antibacterial treatment was expressed in relation to the untreated skin model.

### 2.6. Determination of cytokine levels

Cytokine production was quantified using human interleukin (IL)-6 (Mabtech, Stockholm, Sweden), IL-8 and IL-1 $\alpha$  (R&D Systems, Minneapolis, MN, USA) enzyme-linked immunosorbent assay kits according to the manufacturers' instructions. Optical density was measured using a plate reader (Fluostar Galaxy, BMG, Ortenberg, Germany) operating at 450 nm with reference measurement at 620 nm. IL concentrations were calculated according to a four-parameter fit with lin-log coordinates for optical density (linear scale) and concentration (logarithmic scale).

### 2.7. Determination of gene expression levels

RNA was isolated after removal of the skin models from the inserts using the Qiagen RNeasy Mini Purification Kit (Qiagen, Hilden, Germany). cDNA was obtained by conversion of 20 ng of the isolated RNA using the High Capacity cDNA Reverse Transcription Kit (Life Technologies, Waltham, MA, USA). Real-time polymerase chain reaction (PCR) was carried out using the KAPA SYBR FAST qPCR Kit (KAPABiosystems, Wilmington, MA, USA). For this, 500 nM of each primer and  $2 \times$  SYBR Green-Mix at a total sample volume of 20  $\mu$ L were run on the Rotor-Gene-Q (Qiagen). PCR products were amplified with an initialization step at 95°C for 180 s, followed by 40 cycles of 95°C for 5 s, 60°C for 10 s, and 72°C for 10 s. Expression analysis was based on the  $2^{-\Delta\Delta Ct}$  method [22] using  $\beta$ -actin as the housekeeping gene. Primer sequences are listed in Table 1.

### 2.8. Histological analysis

After fixation in 4% formalin solution, samples were dehydrated stepwise and embedded in paraffin blocks (Merck, Kenilworth, NJ, USA) using standard histology protocols. Samples were sectioned into 4- $\mu$ m-thick sections, mounted on glass slides, rehydrated, and stained with haematoxylin and eosin (Merck) using an automated slide stainer (Leica, Wetzlar, Germany). The stained sections were imaged and photographed using the Axio Scope A.1 (Carl Zeiss, Oberkochen, Germany) coupled to the digital camera Color-View II (Soft Imaging Systems, Berlin, Germany).

**Table 1**  
Primer sequences used for real-time polymerase chain reaction.

Gene name	Primer sequence (5'→3')	
	Forward primer	Reverse primer
Interleukin 6	CCA CCG GGA ACG AAA GAG AA	GAG AAG GCA ACT GGA CCG AA
Interleukin 8	ATG ACT TCC AAG CTG GCC GT	TCC TTG GCA AAA CTG CAC CT
Interleukin 1 $\alpha$	CGC CAA TGA CTC AGA GGA AGA	AGG GCG TCA TTC AGG ATG AA
Human $\beta$ -defensin 2	CCA GCC ATC AGC CAT GAG GGT	GGA GCC CTT TCT GAA TCC GCA
Human $\beta$ -defensin 3	AGC CTA GCA GCT ATG AGG ATC	CTT CGG CAG CAT TTT GCG CCA
Psoriasin (S100A7)	GTC CAA ACA CAC ACA TCT CAC TC	AGC AGG CTT GGC TTC TCA AT
Interleukin 23a	QT00204078 (Quiagen)	
Ribonuclease 7	QT00239463 (Quiagen)	
Toll-like receptor 2	QT00236131 (Quiagen)	
$\beta$ -actin	QT01680476 (Quiagen)	

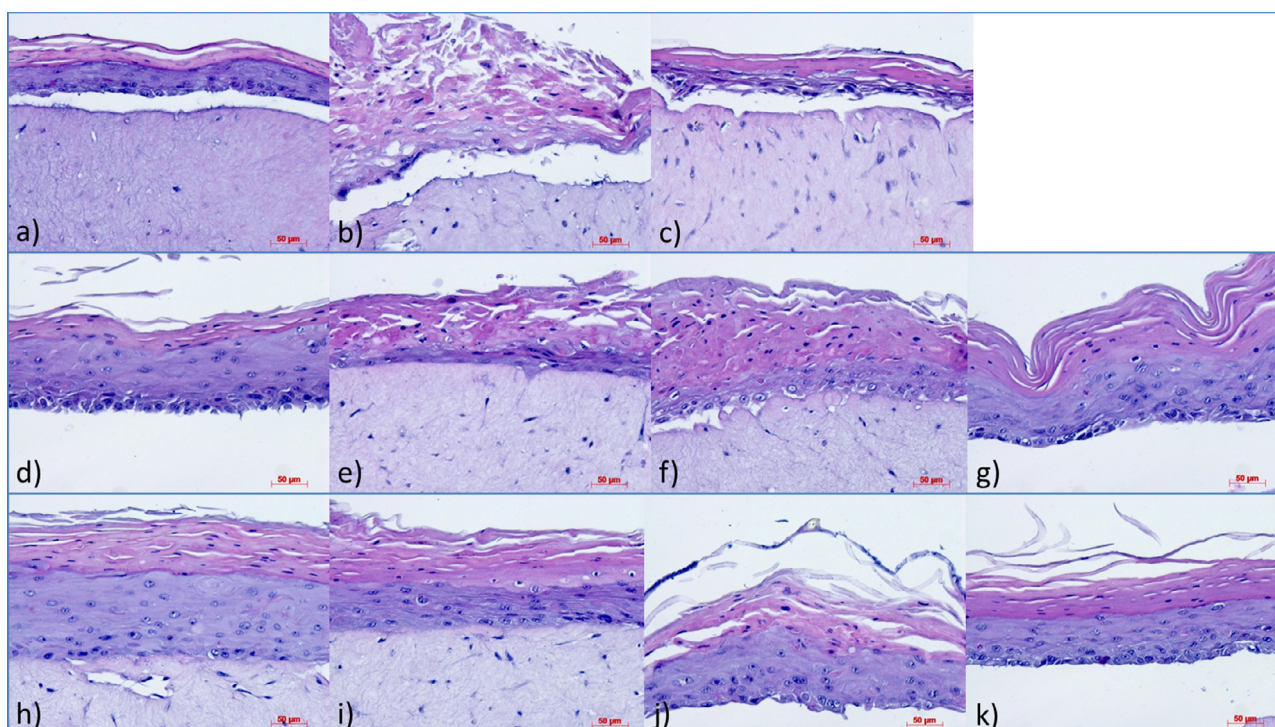


**Fig. 1.** Histology of the infected and treated skin models and staining with haematoxylin and eosin. In contrast to the untreated control (a), incubation with the positive control SDS (b) and infection with *Staphylococcus aureus* (c) distinctly damaged the epidermal layers. After incubation of the untreated and the infected skin models with chlorhexidine digluconate (CHX), polihexanide (PHMB), octenidine dihydrochloride (OCT) and povidone-iodine (PVP-IOD), little influence on the structure of the skin models was observed (d–k). Only the antiseptic control of CHX revealed distinct structural damage of the epidermis (e). Original magnification  $\times 200$ .

## 2.9. Statistics

Experiments were performed in triplicate, and each sample was measured in four replicates. Evaluation was performed using Excel 2010 (Microsoft Corp., Redmond, WA, USA) and OriginLab 9.0 (OriginLab Corp., Northampton, MA, USA). Data are given as mean  $\pm$  standard deviation. Statistical analyses were undertaken using SPSS Version 24 (IBM Corp., Armonk, NY, USA). Determination of statistical significance was calculated using the non-parametric Mann–Whitney U-test with  $P \leq 0.05$ ,  $P \leq 0.01$  and  $P \leq 0.001$  considered to indicate significance.

## 3. Results

The histological structure of the haematoxylin-eosin coloured 3D skin models is shown in Fig. 1. Besides the dermis with fibrob-

lasts embedded in collagen, a fully differentiated epidermis consisting of keratinocytes is visible. In the epidermis, different layers such as the stratum basale, stratum spinosum, stratum granulosum and stratum corneum can be distinguished. Twenty-four-hour incubation of the skin models with the positive controls SDS and *S. aureus* exerted detrimental effects on the epidermis (Fig. 1b,c). After incubation of the untreated and infected skin models with PHMB, CHX, OCT and PVP-IOD, little influence on the structure of the skin models was observed (Fig. 1d–k). Only the antiseptic control of CHX revealed distinct structural damage of the epidermis (Fig. 1e).

Antimicrobial treatment of the *S. aureus* infected skin models revealed excellent bioactivity of all tested antiseptics (Fig. 2). Reduction of the microbial burden after 24 h exceeded 3 log units for all compounds used in this study. The highest antimicrobial effects were observed for CHX, followed by PHMB, PVP-IOD

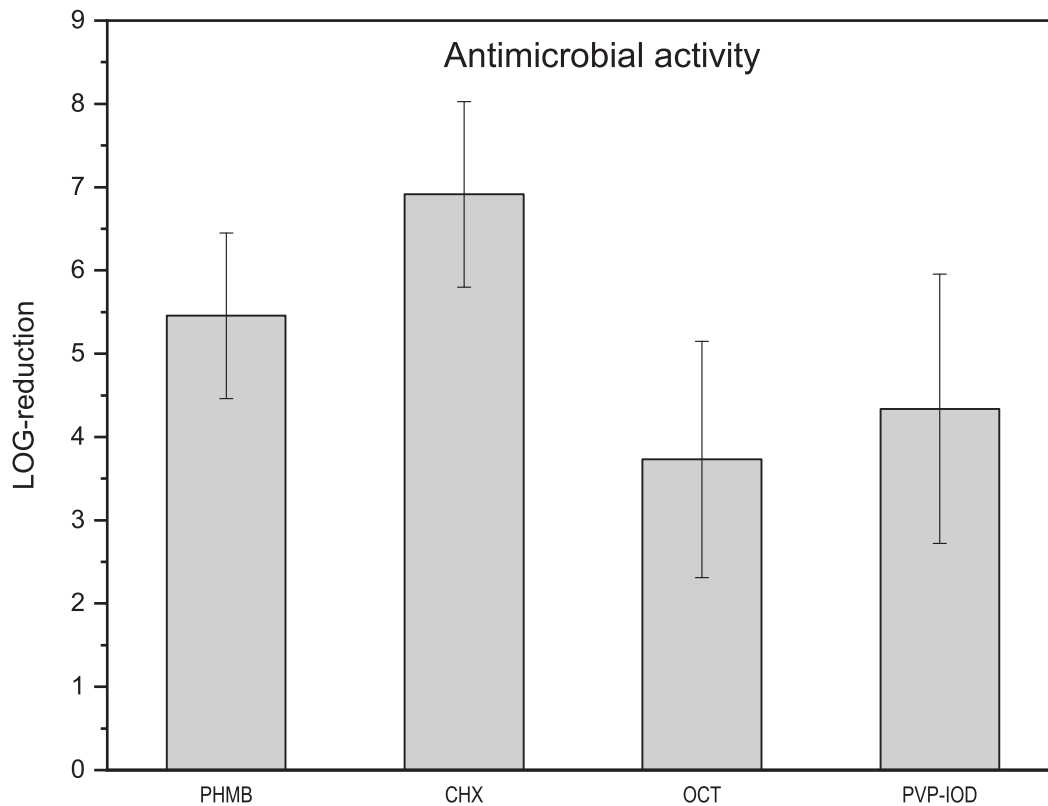


**Fig. 2.** All tested antiseptics exhibited high antimicrobial activity reducing *Staphylococcus aureus* counts after 24 h of treatment. The bacterial burden was calculated by plating serial dilutions of the rinsing solution on Columbia agar and compared with the untreated infected control. Differences between the antiseptics were not statistically significant. Data presented are mean LOG-reduction  $\pm$  standard error ( $n=3$ ). CHX, chlorhexidine digluconate; PHMB, polyhexanide; OCT, octenidine dihydrochloride; PVP-IOD, povidone-iodine.

and OCT. Differences between the antiseptics were not statistically significant.

A strong cytotoxic effect was observed 24 h after infection of the 3D skin models with *S. aureus* (Fig. 3). The leakage of the cytotoxicity marker LDH into the culture medium was comparable to the impact of the positive control SDS. After 24 h of treatment of the infected models with antiseptics, LDH levels were significantly lower with PHMB, OCT and PVP-IOD compared with the infected model. PHMB, OCT and PVP-IOD did not cause an increase in LDH release on their own. Incubation of the infected and uninfected models with CHX resulted in the highest cytotoxic effects compared with the other antiseptics.

Infection of the skin model with *S. aureus* resulted in a distinct inflammatory response after 24 h, with elevated secretion and gene expression levels of IL-6, IL-8, IL-1 $\alpha$  and IL-23 $\alpha$  (Figs. 4 and 5) compared with the untreated control. The inflammatory response was comparable to the impact of SDS as a positive control. Treatment of the infected models with antiseptics reduced the secretion of pro-inflammatory cytokines. In particular for PHMB, the secretion of IL-6, IL-8 and IL-1 $\alpha$  was significantly lower than in the infected control (Fig. 4a,c,e). Similar results were obtained for the relative gene expression levels of IL-6, IL-8 and IL-23 $\alpha$  (Fig. 4b,d, Fig. 5a). For CHX, IL-1 $\alpha$  exhibited a significantly decreased secretion level compared with the infected control (Fig. 4e). IL-6 and IL-8 secretion levels were still elevated due to cytotoxic effects of CHX as demonstrated in the antiseptic's uninfected control (Fig. 4a, c). However, incubation with CHX reduced the gene expression levels in comparison with the infected control for IL-6, IL-8 and IL-23 $\alpha$  (Fig. 4b,d, Fig. 5a). Incubation of the infected models with OCT reduced the secretion of IL-1 $\alpha$  significantly (Fig. 4e). No reduction of IL-6 or IL-8 secretion was observed (Fig. 4a,c). The gene expres-

sion levels after treatment of the infected models with OCT were significantly reduced for IL-6, IL-8 and IL-23 $\alpha$  (Fig. 4b,d, Fig. 5a). PVP-IOD treatment of the infected models reduced the secretion of IL-6 and IL-1 $\alpha$  significantly, but did not reduce the secretion of IL-8 (Fig. 4a,c,e). Gene expression levels of the pro-inflammatory cytokines after treatment with PVP-IOD were significantly reduced for IL-23 $\alpha$  (Fig. 5a).

The expression levels of genes associated with innate immune defence were analysed by real-time PCR, in particular Toll-like receptor 2 (TLR2),  $\beta$ -defensin 3 (DEFB3-1),  $\beta$ -defensin 2 (DEFB2-2), ribonuclease 7 (RNase7) and psoriasin (S100A7). Infection of the 3D skin models with *S. aureus* increased the levels of TLR2 and RNase7 after 24 h (Fig. 5b,f) and decreased S100A7 expression significantly (Fig. 5e). Expression levels of DEFB3-1 and DEFB2-2 were not altered during infection with *S. aureus* (Fig. 5 c,d).

Innate immune defence responses of the infected skin models were found to be increased after treatment with PHMB and PVP-IOD. The effect was most pronounced for treatment of the infected model with PHMB, where gene expression levels of DEFB2-2, DEFB3-1, S100A7 and RNase 7 were significantly increased compared with the infected model, the PHMB uninfected control and the untreated control, respectively (Fig. 5c–f). Gene expression levels were increased more than two-fold. For the PHMB uninfected control, this effect was not visible compared with the untreated control. Treatment of the infected skin model with PVP-IOD resulted in a significant increase in the gene expression levels of human DEFB3-1 and RNase 7 compared with the uninfected, infected and antiseptic controls (Fig. 5c). For CHX and OCT, no significant increase in expression levels of genes associated with innate immune defence after treatment of infected or uninfected models was observed.

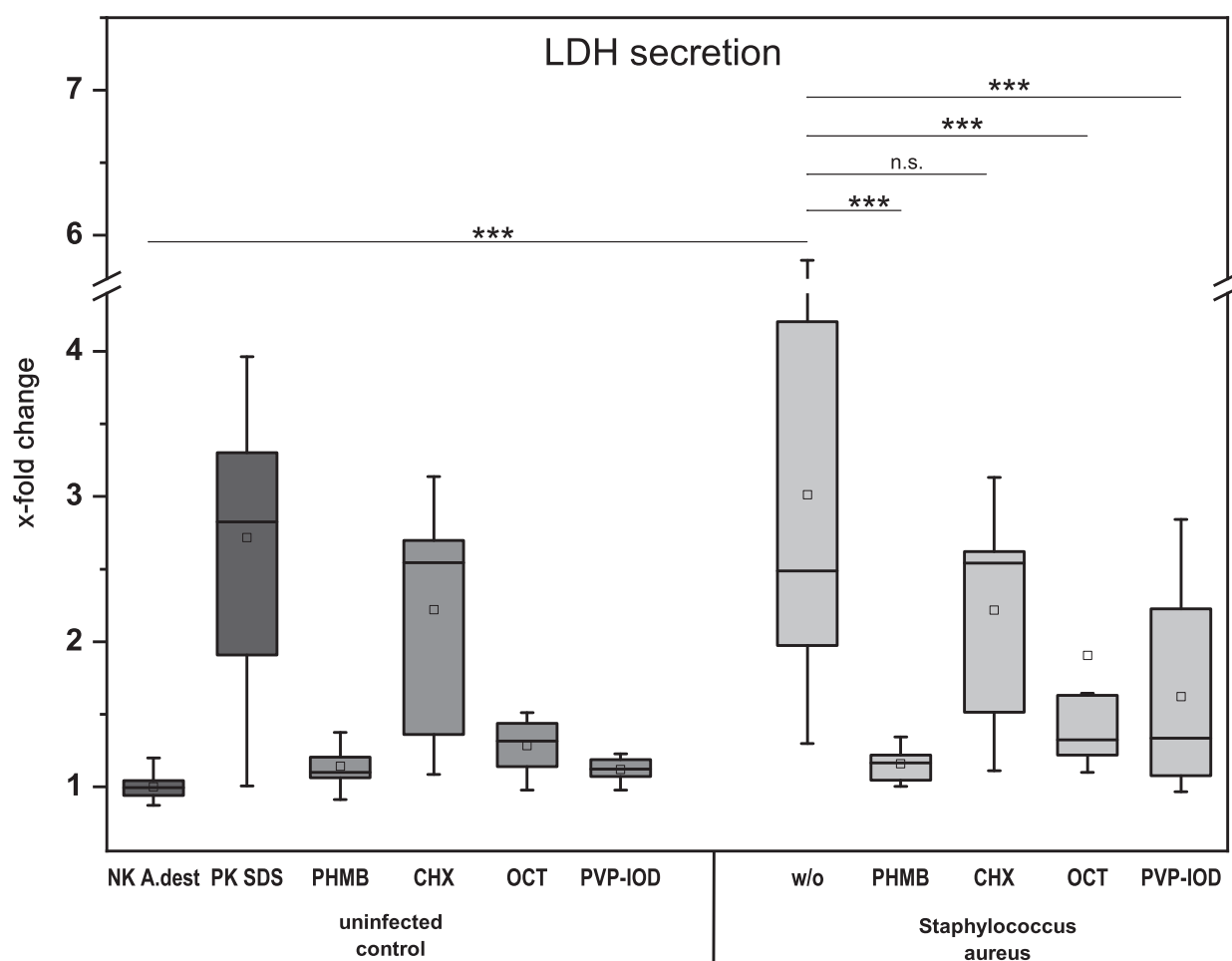


**Fig. 3.** A significant toxic effect after 24 h of incubation with *Staphylococcus aureus* was observed by excretion of the toxicity marker lactate dehydrogenase (LDH). Incubation with the antiseptics polihexanide (PHMB), octenidine dihydrochloride (OCT) and povidone-iodine (PVP-IOD) after infection reduced this toxic effect significantly. Incubation of the infected and uninfected models with chlorhexidine digluconate (CHX) displayed significant cytotoxic effects. PHMB, OCT and PVP-IOD did not cause elevation of LDH release in the uninfected controls.

#### 4. Discussion

Application of topical antiseptics is an important aspect in treating infected acute or chronic wounds and preventing nosocomial infections, especially considering the increasing number of strains resistant to antibiotics (e.g. methicillin-resistant *S. aureus*). For application of antiseptics, evaluation of tissue compatibility and bioactivity against a number of microbes is a prerequisite. Test systems such as 2D cell cultures or planktonic microbes do not reflect the complex interactions between different cell types in human skin and microbes during infection. The development of artificial 3D skin models is a reasonable way to bridge the gap between animal models and cellular monolayers. In this study, an artificial 3D full skin model infected with *S. aureus* was developed for evaluation of bioactivity and biocompatibility of antiseptics.

*S. aureus*, a widespread Gram-positive pathogen, is the most common cause of cutaneous and systemic infections. It may transiently colonize the anterior nares in 20–40% of healthy individuals [23]. Due to its growing resistance to various antibiotics, it is an increasing challenge [24]. In the present study, infection of the 3D skin model with *S. aureus* resulted in distinct detrimental effects. The structure of the dermis was broken up, and secretion of the cytotoxicity marker LDH was enhanced significantly compared with the untreated control. Twenty-four hours after infection, a significant increase in secretion of pro-inflammatory cytokines was ob-

served. Cytokines are small soluble proteins with growth, differentiation and activation functions that act as key modulators of acute and chronic inflammation via a complex cascade of interactions [25]. Cytokines are secreted by a number of cells such as macrophages, monocytes, T cells, mast cells, natural killer cells, endothelial cells, keratinocytes and fibroblasts.

Infection of the 3D skin model with *S. aureus* increased secretion of the cytokines IL-6, IL-8 and IL-1 $\alpha$ , which is in accordance with *S. aureus* infection studies on HaCaT keratinocytes [10], epidermal models [15] and full skin models [26]. The results of cytokine secretion were mirrored in the gene expression analysis. The gene expression level of the pro-inflammatory cytokine IL-23 $\alpha$  was enhanced significantly after infection, which was also observed by Holland et al. [27]. The pro-inflammatory cytokine IL-23 $\alpha$  is involved in activation of IL-17-producing cells such as T cells, mast cells and neutrophils. IL-17 is a key cytokine in defence against *S. aureus* [28].

The antimicrobial innate immune defence is associated with upregulation of pattern recognition receptors such as TLR2 for detection of bacterial lipopeptides. Keratinocytes acting as a physical barrier of the skin and as mediators of the immune system are the major source of antimicrobial peptides (AMPs) such as DEF2-2, DEF3-1, S100A7 and RNase7. AMPs are small, commonly cationic proteins with direct bacteriostatic or bactericidal activity against bacteria such as *S. aureus* [29], which are synthesized

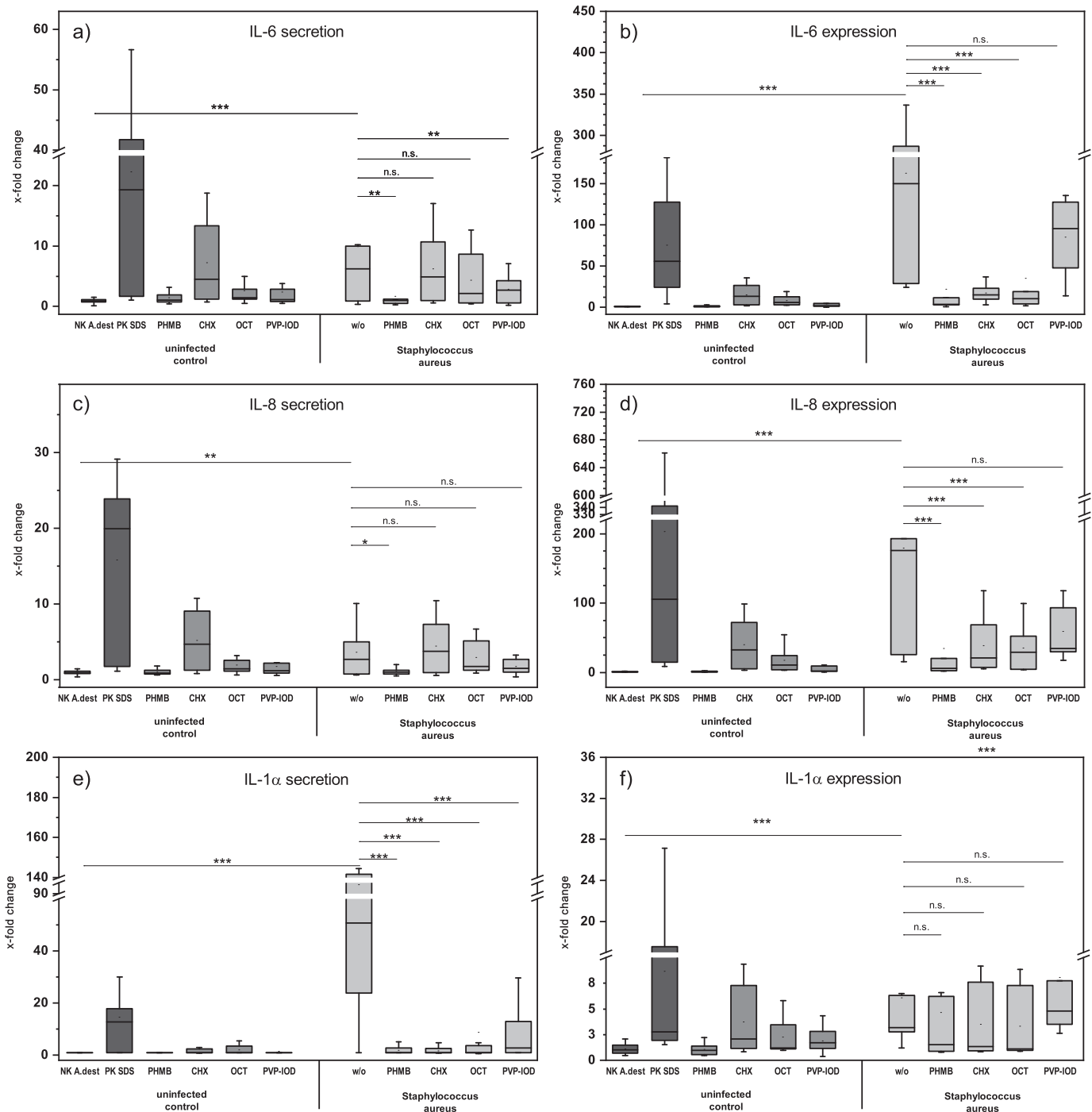


**Fig. 4.** Secretion (a,c,e) and relative gene expression levels (b,d,f) of the cytokines IL-6, IL-8 and IL-1 $\alpha$  revealed significant damage of the skin models after 24 h of incubation with *Staphylococcus aureus*. Treatment with the tested antiseptics after infection reduced the damage caused by *S. aureus* significantly. Secretion was measured by enzyme-linked immunosorbent assay, and the relative gene expression levels compared with the non-treated control were determined by real-time polymerase chain reaction. Asterisks indicate significant deviations from the respective control: \* $P < 0.05$ ; \*\* $P < 0.01$ ; \*\*\* $P < 0.001$ . CHX, chlorhexidine digluconate; PHMB, polyhexanide; OCT, octenidine dihydrochloride; PVP-IOD, povidone-iodine.

by keratinocytes, epithelial cells of the eccrine glands, sebocytes and mast cells [30]. Production of AMPs is stimulated through TLR signalling. In the authors' studies, the gene expression of TLR2 and RNase7 was significantly upregulated after *S. aureus* infection, S100A7 expression was downregulated, and no difference was observed in DEFB2-2 and DEFB3-1 expression compared with the untreated control. Previous studies on *S. aureus* infection of full skin models and skin explants also demonstrated increased gene expression or secretion of TLR2 and RNase7 [26,27,31]. RNase7

is an AMP with a broad antimicrobial spectrum, and one of the major AMPs involved in cutaneous *S. aureus* defence [31]. In the present study, no increase in gene expression of DEFB2-2 and DEFB3-1 was observed after *S. aureus* infection. These findings contrast with previously published data, where gene expression of DEFB2-2 and DEFB3-1 after *S. aureus* infection was found to be upregulated *in vitro* using keratinocyte monolayers [32,33], full skin models [26] and testing patients infected with *S. aureus* *in vivo* [34].

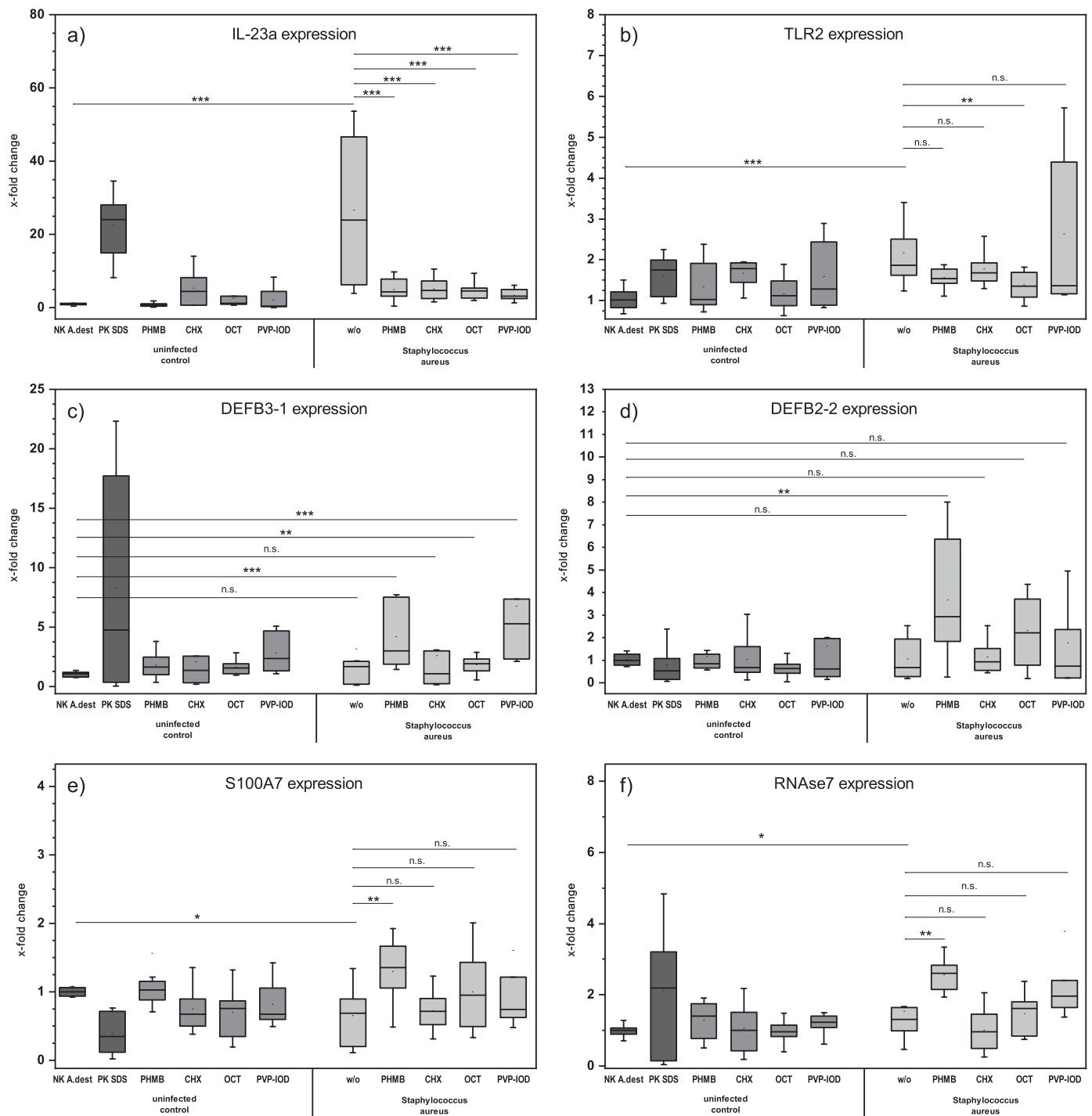


**Fig. 5.** Relative gene expression levels of the pro-inflammatory cytokine IL-23a and Toll-like receptor 2 (TLR2) demonstrated significant damage of the skin models 24 h after infection with *Staphylococcus aureus*. Treatment of the infected three-dimensional skin models with the antiseptics decreased the detrimental effects caused by *Staphylococcus aureus* significantly. No or little increase in the gene expression level of the antimicrobial peptides human  $\beta$ -defensin 1 (DEFB3-1), human  $\beta$ -defensin 2 (DEFB2-2), psoriasin (S100A7) and ribonuclease 7 (RNase7) after infection was observed. The antiseptics augmented immune responses of the infected skin models significantly. The relative gene expression levels compared with the non-treated control were determined by real-time polymerase chain reaction. Asterisks indicate significant deviations from the respective control: \* $P < 0.05$ ; \*\* $P < 0.01$ ; \*\*\* $P < 0.001$ . CHX, chlorhexidine digluconate; PHMB, polyhexanide; OCT, octenidine dihydrochloride; PVP-IOD, povidone-iodine.

This study demonstrated strong bioactivity of the antiseptics PHMB, CHX, OCT and PVP-IOD in the infected 3D skin models, and good biocompatibility of PHMB, PVP-IOD and OCT in the uninfected models at application-relevant concentrations. Cytotoxic damages were only observed for CHX. Due to its cytotoxic effects, the risks of anaphylactic reactions and the progressive development of resistant microbes, CHX has now generally been replaced in wound treatment [35]. The highest bioactivity in combination

with the best biocompatibility was observed for PHMB. This is in accordance with Hirsch et al. [1]. Mueller and Kramer [9] defined the biocompatibility index of a number of antiseptics by measuring the antibacterial activity against *Escherichia coli* and *S. aureus* and, in parallel, the cytotoxicity on cultured murine fibroblasts after incubation for 30 min. They stated a rank order for biocompatibility of OCT>PHMB>CHX>PVP-IOD, with OCT and PHMB yielding biocompatibility index values >1 meaning that these substances are

more toxic to the tested micro-organisms than the murine fibroblasts [15].

Application of the tested antiseptics to the infected 3D skin models prevented the strong damage that was observed 24 h after *S. aureus* infection in the skin models without treatment. LDH secretion of the antiseptic-treated infected models was significantly lower than in the infected model and comparable to the uninfected controls. Secretion of the pro-inflammatory cytokine IL-1 $\alpha$  was also significantly lower after application of the four tested antiseptics. For IL-6 secretion, this effect was observed for PHMB and PVP-IOD, and for IL-8 secretion, it was observed for PHMB alone. Gene expression levels of IL-6, IL-8 and IL-23 $\alpha$  indicated a similar reaction. For IL-1 $\alpha$ , significant differences in cytokine secretion between the infected model and the antiseptic-treated infected model were observed, but no significant differences were seen in IL-1 $\alpha$  gene expression. The biologically active IL-1 $\alpha$  is stored in keratinocytes, and is one of the important proteins that are released in the early stage of immune response to microbial attack [29]. Hence, differences in significance between IL-1 $\alpha$  secretion and gene expression can be explained by the timeline of the immune response, revealing that IL-1 $\alpha$  is quickly released upon infection. This cytokine release can be prevented by application of antiseptics.

Surprisingly, application of PHMB to the *S. aureus*-infected 3D skin models improved the innate immune reactivity of the model, and gene expression levels of DEFB2-2, DEFB3-1, S100A7 and RNase7 were significantly upregulated. To the authors' knowledge, this is the first study to report such an effect. Addition of PHMB to the uninfected models did not evoke such a response. A possible explanation for this observation is the destruction of the microbial cells by PHMB, and subsequent presentation of an increased number of microbial recognition sites to the human cells, leading to an augmented innate immune response of the skin model. Due to the structural similarities to AMPs, PHMB can incorporate into bacterial cell membranes and kill bacteria by permeabilizing the bacterial membrane and inducing cell lysis [36]. An increased immune response of the human cells was not observed after application of CHX, OCT or PVP-IOD to the infected 3D skin model. However, the observations are in accordance with in-vitro [3,4,37] and in-vivo studies [38,39] that show improved wound healing after treatment with PHMB. Hence, PHMB is the recommended antiseptic for treating critically colonized wounds and burns, and for decontamination of chronic wounds [35].

## 5. Conclusions

This study demonstrates the suitability of the developed *S. aureus*-infected artificial skin model as a tool to investigate the immune response of human cells in a complex 3D structure to microbial infections. It is also appropriate for evaluating the bioactivity and biocompatibility of antiseptics. The reproducible structure with low sample-to-sample variation is advantageous compared with other test systems like ex-vivo models or animal testing. Using the *S. aureus*-infected artificial skin model, it could be shown that the detrimental effects caused by *S. aureus* infection can be prevented by antiseptic treatment. Moreover, the biocompatibility of application-relevant concentrations of antiseptics could be demonstrated here. Hence, the developed infection model provides a promising tool to evaluate new targets for antimicrobial strategies due to improved in-vitro to in-vivo extrapolation capability of the test results.

## Acknowledgements

The authors wish to thank Doreen Winter for her expert technical assistance.

## Funding

This research was supported by KF3071902LW3 grant from Arbeitsgemeinschaft Industrieller Forschungsvereinigungen. The funding source had no involvement in study design, analysis or publication of data.

## Competing interests

None declared.

## Ethical approval

Not required.

## References

- [1] Hirsch T, Koerber A, Jacobsen F, Dissemund J, Steinau HU, Gatermann S, et al. Evaluation of toxic side effects of clinically used skin antiseptics in vitro. *J Surg Res* 2010;164:344–50.
- [2] Koburger T, Hubner NO, Braun M, Siebert J, Kramer A. Standardized comparison of antiseptic efficacy of triclosan, PVP-iodine, octenidine dihydrochloride, polyhexanide and chlorhexidine digluconate. *J Antimicrob Chemother* 2010;65:1712–19.
- [3] Roth C, Beule AG, Kramer A, Hosemann W, Kohlmann T, Scharf C. Response analysis of stimulating efficacy of polyhexanide in an in vitro wound model with respiratory ciliary epithelial cells. *Skin Pharmacol Physiol* 2010;23(Suppl.):35–40.
- [4] Wiegand C, Abel M, Kramer A, Mueller G, Ruth P, Hipler UC. Proliferationsförderung und Biokompatibilität von Polihexanid. *GMS Krankenhaushygiene interdisziplinär*. Berlin, Germany; 2007.
- [5] Faria G, Cardoso CRB, Larson RE, Silva JS, Rossi MA. Chlorhexidine-induced apoptosis or necrosis in L929 fibroblasts: a role for endoplasmic reticulum stress. *Toxicol Appl Pharmacol* 2009;234:256–65.
- [6] Giannelli M, Chellini F, Margheri M, Tonelli P, Tani A. Effect of chlorhexidine digluconate on different cell types: a molecular and ultrastructural investigation. *Toxicol in Vitro* 2008;22:308–17.
- [7] Liu XH, Chen GG, Vlantis AC, Tse GM, van Hasselt CA. Iodine induces apoptosis via regulating MAPKs-related p53, p21, and Bcl-xL in thyroid cancer cells. *Molec Cell Endocrinol* 2010;320:128–35.
- [8] Chindera K, Mahato M, Kumar Sharma A, Horsley H, Kloc-Muniak K, Kamaruzaman NF, et al. The antimicrobial polymer PHMB enters cells and selectively condenses bacterial chromosomes. *Sci Rep* 2016;6:23121.
- [9] Müller G, Kramer A. Biocompatibility index of antiseptic agents by parallel assessment of antimicrobial activity and cellular cytotoxicity. *J Antimicrob Chemother* 2008;61:1281–7.
- [10] Wiegand C, Abel M, Ruth P, Hipler UC. HaCaT keratinocytes in co-culture with *Staphylococcus aureus* can be protected from bacterial damage by polyhexanide. *Wound Rep Regen* 2009;17:730–8.
- [11] Haycock JW. 3D cell culture: a review of current approaches and techniques. *Meth Molec Biol* 2011;695:1–15.
- [12] Eberhardt K, Matthaues C, Winter D, Wiegand C, Hipler UC, Diekmann S, et al. Raman and infrared spectroscopy differentiate senescent from proliferating cells in a human dermal fibroblast 3D skin model. *Analyst* 2017;142:4405–14.
- [13] de Breij A, Haisma EM, Rietveld M, El Ghalbzouri A, van den Broek PJ, Dijkshoorn L, et al. Three-dimensional human skin equivalent as a tool to study *Acinetobacter baumannii* colonization. *Antimicrob Agents Chemother* 2012;56:2459–64.
- [14] Müller G, Langer J, Siebert J, Kramer A. Residual antimicrobial effect of chlorhexidine digluconate and octenidine dihydrochloride on reconstructed human epidermis. *Skin Pharmacol Physiol* 2014;27:1–8.
- [15] Son ED, Kim H-J, Park T, Shin K, Bae I-H, Lim K-M, et al. *Staphylococcus aureus* inhibits terminal differentiation of normal human keratinocytes by stimulating interleukin-6 secretion. *J Dermatol Sci* 2014;74:64–71.
- [16] Lerebour G, Cupferman S, Bellon-Fontaine MN. Adhesion of *Staphylococcus aureus* and *Staphylococcus epidermidis* to the Episkin® reconstructed epidermis model and to an inert 304 stainless steel substrate. *J Appl Microbiol* 2004;97:7–16.
- [17] Haisma EM, de Breij A, Chan H, van Dissel JT, Drijfhout JW, Hiemstra PS, et al. LL-37-derived peptides eradicate multidrug-resistant *Staphylococcus aureus* from thermally wounded human skin equivalents. *Antimicrob Agents Chemother* 2014;58:4411–19.
- [18] Holland DB, Bojar RA, Jeremy AHT, Ingham E, Holland KT. Microbial colonization of an in vitro model of a tissue engineered human skin equivalent – a novel approach. *FEMS Microbiol Lett* 2008;279:110–15.
- [19] Popov L, Kovalski J, Grandi G, Bagnoli F, Amieva MR. Three-dimensional human skin models to understand *Staphylococcus aureus* skin colonization and infection. *Front Immunol* 2014;5:41.
- [20] Shepherd J, Douglas I, Rimmer S, Swanson L, MacNeil S. Development of three-dimensional tissue-engineered models of bacterial infected human skin wounds. *Tissue Eng Part C: Meth* 2009;15:475–84.

- [21] Wiegand C, Fink S, Beier O, Horn K, Pfuch A, Schimanski A, et al. Dose- and time-dependent cellular effects of cold atmospheric pressure plasma evaluated in 3D skin models. *Skin Pharmacol Physiol* 2016;29:257–65.
- [22] Pfaffl MW. Real-time RT-PCR: Neue Ansätze zur exakten mRNA Quantifizierung. *BIOspektrum* 2004;1:92–5.
- [23] Chiller K, Selkin BA, Murakawa GJ. Skin microflora and bacterial infections of the skin. *J Investig Dermatol Symp Proc* 2001;6:170–4.
- [24] McCaig LF, McDonald LC, Mandal S, Jernigan DB. *Staphylococcus aureus*-associated skin and soft tissue infections in ambulatory care. *Emerg Infect Dis* 2006;12:1715–23.
- [25] Turner MD, Nedjai B, Hurst T, Pennington DJ. Cytokines and chemokines: at the crossroads of cell signalling and inflammatory disease. *Biochim Biophys Acta* 2014;1843:2563–82.
- [26] Haisma EM, Rietveld MH, de Breij A, van Dissel JT, El Ghalbzouri A, Nibbering PH. Inflammatory and antimicrobial responses to methicillin-resistant *Staphylococcus aureus* in an in vitro wound infection model. *PLoS One* 2013;8:e82800.
- [27] Holland DB, Bojar RA, Farrar MD, Holland KT. Differential innate immune responses of a living skin equivalent model colonized by *Staphylococcus epidermidis* or *Staphylococcus aureus*. *FEMS Microbiol Lett* 2009;290:149–55.
- [28] Cua DJ, Tato CM. Innate IL-17-producing cells: the sentinels of the immune system. *Nat Rev Immunol* 2010;10:479–89.
- [29] Hill PB, Imai A. The immunopathogenesis of staphylococcal skin infections – a review. *Comparat Immunol Microbiol Infect Dis* 2016;49:8–28.
- [30] Cordes J, Wittersheim M, Harder J, Glaser R. [The skin's own antibiotics. Important features of antimicrobial peptides for clinical practice]. *Der Hautarzt; Zeitschrift für Dermatologie, Venerologie, und verwandte Gebiete* 2014;65: 50–55.
- [31] Simanski M, Dressel S, Gläser R, Harder J. RNase 7 protects healthy skin from *Staphylococcus aureus* colonization. *J Investig Dermatol* 2010;130:2836–8.
- [32] Ommori R, Oujii N, Mizuno F, Kita E, Ikada Y, Asada H. Selective induction of antimicrobial peptides from keratinocytes by staphylococcal bacteria. *Microb Pathogen* 2013;56:35–9.
- [33] Kisich KO, Howell MD, Boguniewicz M, Heizer HR, Watson NU, Leung DYM. The constitutive capacity of human keratinocytes to kill *Staphylococcus aureus* is dependent on  $\beta$ -defensin 3. *J Investig Dermatol* 2007;127:2368–80.
- [34] Zanger P, Holzer J, Schleucher R, Scherbaum H, Schitteck B, Gabrysich S. Severity of *Staphylococcus aureus* infection of the skin is associated with inducibility of human beta-defensin 3 but not human beta-defensin 2. *Infect Immun* 2010;78:3112–17.
- [35] Kramer A, Dissemmond J, Kim S, Willy C, Mayer D, Papke R, et al. Consensus on wound antiseptics: update 2018. *Skin Pharmacol Physiol* 2018;31:28–58.
- [36] Moore K, Gray D. Using PHMB antimicrobial to prevent wound infection. *Wounds UK* 2007;3:96–102.
- [37] Kramer A, Roth B, Müller G, Rudolph P, Klocker N. Influence of the antiseptic agents polyhexanide and octenidine on FL cells and on healing of experimental superficial aseptic wounds in piglets. A double-blind, randomised, stratified, controlled, parallel-group study. *Skin Pharmacol Physiol* 2004;17:141–6.
- [38] Bellingeri A, Falciani F, Traspardini P, Moscatelli A, Russo A, Tino G, et al. Effect of a wound cleansing solution on wound bed preparation and inflammation in chronic wounds: a single-blind RCT. *J Wound Care* 2016;160(25):162–6.
- [39] Marquardt C, Koppes P, Krohs U, Mares A, Paglinawan R, Höfer D, et al. Vakuumtherapie mit PHMB Gaze zur Behandlung postoperativer subkutaner Bauchdeckeninfektionen. *Coloproctology* 2014;36:364–9.